Surface Fluxes under Weak Wind Conditions

Final Report

Larry Mahrt

College of Oceanic and Atmospheric Sciences
Oregon State University
Corvallis, OR 97331
phone: (541) 737-5691 fax: (541) 737-2540
email: mahrt@coas.oregonstate.edu
Grant #: N00014-01-1-0084
http://blg.oce.orst.edu/cblast-weakwind

31 August 2005

REPORT DOCUMENTATION PAGE

Form Approved
OMB No. 0704-0188

1. AGENCY USE ONLY (Leave blank)	2. REPORT DATE	3. REPORT TYPE AND DATES COVERED
	9-21-05	Final 11-17-00 to 12-31-05

4. TITLE AND SUBTITLE
Surface Fluxes and Wind-Wave Interactions in Weak Wind Conditions

5. FUNDING NUMBERS
N00014-01-1-0084

6. AUTHOR(S)
Larry J. Mahrt

7. PERFORMING ORGANIZATION NAME(S) AND ADDRESS(ES)
Oregon State University
Corvallis, OR 97331

8. PERFORMING ORGANIZATION REPORT NUMBER
N01430

9. SPONSORING/MONITORING AGENCY NAME(S) AND ADDRESS(ES)
ONR

10. SPONSORING/MONITORING AGENCY REPORT NUMBER

11. SUPPLEMENTARY NOTES

12a. DISTRIBUTION/AVAILABILITY STATEMENT
Unlimited Public Access

12b. DISTRIBUTION CODE

13. ABSTRACT *(Maximum 200 words)*

We have examined each of a number of physical mechanisms thought to be important for weak wind conditions by collecting aircraft and tower data in both open-ocean and fetch-limited conditions. This investigation relied on eddy-correlation data from both aircraft and towers. Our contention is that existing analyses for weak wind situations are often strongly influenced by observational errors and analyses problems, which have been given special emphasis in this study.

14. SUBJECT TERMS			15. NUMBER OF PAGES
			16. PRICE CODE
17. SECURITY CLASSIFICATION OF REPORT	18. SECURITY CLASSIFICATION OF THIS PAGE	19. SECURITY CLASSIFICATION OF ABSTRACT	20. LIMITATION OF ABSTRACT

LONG-TERM GOAL

The long-term goals included re-examination of the applicability of Monin-Obukhov similarity theory and the Charnock formulation over the sea, the influence of wave state on such relationships and the vertical structure of the marine boundary layer in response to changes of SST.

OBJECTIVES

We have examined each of a number of physical mechanisms thought to be important for weak wind conditions by collecting aircraft and tower data in both open-ocean and fetch-limited conditions. This investigation relied on eddy-correlation data from both aircraft and towers. Our contention is that existing analyses for weak wind situations are often strongly influenced by observational errors and analyses problems, which have been given special emphasis in this study.

APPROACH

Our analysis has concentrated primarily on the LongEZ eddy-correlation data in the CBLAST Weak Wind Pilot Experiment 2001. We also have employed eddy correlation on the CBLAST WHOI ASIT tower. The processed data has been analyzed toward the goal of improving physical understanding and parameterization of sea surface fluxes and have been provided to LES and larger-scale modeling groups. The long-term goal of including the effect of wave state is still under investigation.

RESULTS

The publications below are based on observations from both the CBLAST Weak Wind and SHOWEX experiments. We have included two of the manuscripts in full as part of this report. "Fluxes measured from moving platforms" evaluated errors associated with fluctuations in height of the light-weight LongEz aircraft and found such errors to be important only in very stable conditions. "Flow adjustments across sea-surface temperature changes" examined the response of the marine boundary layer to strong SST variations and found that such large spatial changes of SST can reverse the sign of the area-averaged flux-gradient relationship. This work was carried out using SHOWEX data as a precursor to analyzing the data from the delayed CBLAST Weak Wind experiment. This analysis was extended to include data from the CBLAST Weak Wind Experiment in "Atmospheric response to sea-surface temperature variability".

This work was further extended in the not-yet-submitted manuscript "Aircraft and tower observations of air-sea fluxes: bulk modeling, and sea-surface temperature variability", which is now summarized. A bulk flux model with no wave state information, similar to that used to parameterize air-sea fluxes in most large scale atmospheric models, was evaluated using the aircraft data in CBLAST Weak Wind, as well as supplementary data from SHOWEX. While we cannot rule out the possibility that the measurements underestimate surface fluxes, the differences between bulk and observed latent heat fluxes appear to be too large to be fully explained by measurement problems.

With weak to moderate winds, the observed fluxes of latent heat were systematically smaller than predicted by the model. The more efficient transfer of heat compared to moisture for weak to moderate winds, as reflected by the roughness lengths, is consistent with the increased importance of temperature, as compared to moisture, in the buoyancy

generation of turbulence in these datasets. The ratio of the thermal roughness length to that for moisture is of order 10 except for the strongest wind speed conditions associated with wave breaking, where it decreases to order 0.1. The enhanced moisture flux over breaking waves is coincident with strong advection of cold dry air from the continent.

The momentum, sensible heat and latent heat fluxes respond strongly to SST changes, which exceed 1 C in amplitude on the 8-km scale (difference between two adjacent 4-km averages of SST). When the change in SST is less than this value, the response of the fluxes is not significant. A larger number of repeat passes over the same SST feature would be required to extend this analysis to shorter scales. A case study of flow from cold to warm water shows that acceleration of the low-level mean wind over the warm pool appears to be related to the decrease in vertical stress divergence associated with a much deeper boundary layer over the warm water.

Aircraft soundings indicate that the depth of the marine boundary layer is poorly predicted by existing formulations ("Evaluating formulations of stable boundary-layer height"). Inclusion of additional information, such as surface roughness, lead to only modest improvements.

PUBLICATIONS

Mahrt, L., D. Vickers, W. Drennan, H. Graber and T. Crawford, 2005: Fluxes measured from moving platforms. *J. Atm. and Oc. Tech. 22,* 857-865. [published, refereed]

Vickers, D. and L. Mahrt, 2004: Evaluating formulations of stable boundary-layer height. *J. Appl. Meteor.*, 43, 1736-1749 [published, refereed]

Mahrt, L., Vickers, D. and E. Moore, 2004: Flow adjustments across sea-surface temperature changes. *Bound. Layer Meteor.* 111, 553-564. [published, refereed]

Vickers, D. and L. Mahrt, 2004: Atmospheric response to sea-surface temperature variability. 16th Boundary Layer -Turbulence Conference. American Meteorological Society. Portland, Maine, August 2004.

Sun, J., S.P. Burns, D. Vandemark, M. A. Donelan, L. Mahrt, T. Crawford, G. Crescenti and J. R. French, 2005: Measurement of directional wave spectra using aircraft laser altimeters. *Atmos. Oc. Tech,* 111, 866-882. [published, refereed].

Vickers, D. and L. Mahrt, 2005: Aircraft and tower observations of air-sea fluxes: bulk modeling, and sea-surface temperature variability. [manuscript]

Displacement measurement errors from moving platforms

L. Mahrt and Dean Vickers

COAS
Oregon State University
Corvallis, OR 97331 USA
mahrt@coas.oregonstate.edu

William M. Drennan and Hans C. Graber

Rosenstiel School of Marine and Atmospheric Science
University of Miami
Miami, FL 33149, U.S.A.

Timothy L. Crawford
Air Resources Laboratory
NOAA
Idaho Falls, ID, 83402, USA

Abstract

Errors in eddy correlation measurements from moving platforms (aircraft, ships, buoys, blimps, tethered balloons and kites) include contamination of the measured fluctuations by superficial fluctuations associated with vertical movement of the platform in the presence of mean vertical gradients. Such errors occur even with perfect removal of the motion of the platform. These errors are investigated here from eddy correlation data collected from the LongEZ research aircraft and ASIS buoy during the SHOaling Waves EXperiment.

1 Introduction

Except for towers, eddy correlation measurements of turbulent fluxes are generally made from moving platforms such as aircraft, buoys, ships and suspended platforms from tethered balloons, blimps, kites and aircraft. Errors in the measured velocity fluctuations occur due to incomplete removal of the platform motion, normally recorded with accelerometers, gyroscopes and differential GPS (Lenschow, 1986; Edson et al., 1998). Improvements in such systems are constantly reducing the errors associated with platform motion. Even with complete removal of platform motion, eddy correlation errors still occur due to the fact that the time series is not collected at a constant height above the mean surface and mean vertical gradients are normally not zero, particularly near the surface (Figure 1). Examples of vertical displacement are shown for the aircraft and buoy in Figure 2. As a result of the vertical platform displacements, superficial fluctuations may be generated by

the variation of the height of the measurement platform due to the vertical mean gradients. These errors were briefly examined in Lenschow (1973) and Vickers and Mahrt (1997), but otherwise are generally not considered in the literature. This study examines such errors in more detail. The errors due to vertical platform displacement are just one of a number of instrumental and sampling errors contaminating eddy correlation measurements from fixed or moving platforms (Moore, 1986; Mann and Lenschow, 1994; Mahrt, 1998 and Massman, 2000).

2 The data

For aircraft data, the errors due to vertical platform displacement are most easily examined over water where variations of surface elevation do not complicate the definition of height above ground. This study analyzes eddy correlation data collected from the LongEZ research aircraft over Atlantic coastal water off the Outer Banks near Duck, North Carolina during the SHOaling Waves EXperiment (SHOWEX) in March 1999 and November-December 1999 (Crescenti et al., 1999; French et al., 2000; Sun et al., 2001; Mahrt et al., 2001) using low-level aircraft data from 37 flights on 35 days at an average height of 15 m above the sea surface. The LongEZ is able to fly at this very low level for several hours at a time.

Fluxes are computed for 2 km segments of the aircraft legs using unweighted averaging. For a wind of $5ms^{-1}$, this volume of air would pass a stationary platform in about 7 min. Records with negative moisture flux, upward momentum flux (presumably driven by swell), and flight levels above 25 m are excluded since some of the calculations will employ surface-layer similarity theory. Records are excluded where the absolute value of z/L exceeds

five where fluxes may be strongly contaminated by flux sampling errors and where similarity theory is suspect. Here, L is the Obukhov length and z is the distance above the mean surface height. When computing bin-averaged values of ratios, such as the relative flux error (Section 5), for different intervals of stability, z/L, the values of the numerator and denominator are averaged first and then the ratio is computed. This procedure avoids ratio averaging problems where a few very large values of the ratio, due to small denominators, can dominate the average of the ratio. For some calculations, the data will be divided into stable and unstable classes. Here we exclude near neutral cases where the magnitude of z/L is less than 0.001.

The ASIS, or Air-Sea Interaction Spar buoy (Graber et al. 2000), is a partial surface follower, essentially following waves with periods longer than 8 s. This latter property allows measurements within several metres of the interface in most conditions. The data used here are from the 'ROMEO' buoy during the SHOWEX experiment of autumn 1999. ROMEO is equipped with a 3-axis Gill R2A sonic anemometer, located on top of a mast at roughly 6m above mean sea level. The buoy is also equipped with a full motion package, allowing the measured wind velocities to be corrected for the motion of the platform. The instantaneous height of the anemometer above the surface is calculated from a capacitance wave staff positioned directly below the anemometer. For the calculations in this study, 30-minute records were selected every ten hours to provide a more manageable data set and to represent a cross-section of conditions during the 38 day deployment: $1 < U < 15 ms^{-1}$ and $-2 < z/L < 1$. The fluxes are computed with simple unweighted averaging (equal weighting of all points).

3 Platform displacement errors

Aircraft vertical displacement from a constant height above the surface is induced by turbulent updrafts and downdrafts and perhaps fluctuations of lift due to horizontal velocity fluctuations. Vertical displacement of buoys and ships is controlled by the surface wave field. The artificial fluctuations due to the height-variation of the observational platform for arbitrary variable ϕ (Figure 1) can be estimated as

$$\delta\phi(z') = z'(t)\frac{\partial\overline{\phi}}{\partial z} \tag{1}$$

where $\delta\phi(z')$ is the change of variable ϕ due to the vertical displacement of the platform from its mean elevation

$$z'(t) = z(t) - Z \tag{2}$$

where Z is the time-averaged height of the platform and $z(t)$ is the instantaneous height of the platform. Then any variable measured from the platform can be expressed as

$$\phi(z', t) = \phi(Z, t) + z'(t)\frac{\partial\overline{\phi}}{\partial z} \tag{3}$$

where $\phi(Z, t)$ is the desired instantaneous value measured at a fixed height. We will assume that the vertical mean gradient does not change significantly across the layer defined by $z'(t)$ and assume that the flow is stationary.

The vertical gradients may be large near the surface, resulting in significant artificial fluctuations, even if the change of platform vertical position is small. Are such artificial fluctuations sufficiently correlated with vertical velocity fluctuations to significantly alter the computed flux? To investigate

this issue, we expand the measured vertical flux as

$$\overline{w'(z,t)\phi'(z,t)} = \overline{w'(Z,t)\phi'(Z,t)} + \overline{w'(Z,t)\delta\phi(z')} + \overline{\delta w(z')\phi'(Z,t)} + \overline{\delta w(z')\delta\phi(z')} \tag{4}$$

where the overbar is a simple unweighted average in order to satisfy Reynolds averaging. The first term on the right hand side is the true vertical flux required for use in the basic conservation equation for $\overline{\phi}$. The remaining three terms on the right hand side are error terms. The last two error terms on the right hand side are related to heterogeneity of the mean flow through mass continuity in that artificial fluctuations of vertical velocity are proportional to $\partial\overline{w}/\partial\overline{z}$ (Eq. 1). These terms vanish for homogenous flow. Even if the platform was motionless with no vertical displacement, the estimate of the first term on the right hand side of Eq. 4 from finite records contains a random flux error due to variability of the turbulence.

4 Vertical velocity correlation term

The second term on the right hand side is due to the correlation between the vertical velocity fluctuations and the artificial fluctuations of ϕ. Estimating the $\delta\phi(z')$ from Eq. 1, this term becomes

$$\overline{w'(Z,t)\delta\phi(z')} = \overline{w'(Z,t)z'(t)}\frac{\partial\overline{\phi}}{\partial z}. \tag{5}$$

To numerically estimate this error term, $w'(Z,t)$ is approximated by $w'(z',t)$. Below, $\phi'(Z,t)$ will be approximated by $\phi'(z',t)$. Such approximations correspond to only higher order errors, which are small compared to $\overline{w'(Z,t)\delta\phi(z')}$ provided that z' is not too large.

The vertical gradient, $\partial\overline{\phi}/\partial z$, can be estimated in two ways. In the first approach, it is estimated by regressing $\phi'(z',t)$ on z. A potential difficulty of this "regression" approach is that the platform height might be correlated with the turbulence itself, in which case the estimated value of $\partial\overline{\phi}/\partial z$ is contaminated by turbulent fluctuations. For example, the aircraft is displaced by vertical velocity fluctuations while waves simultaneously displace the buoy and induce atmospheric velocity fluctuations.

In the second approach, the vertical gradient $(\partial\overline{\phi}/\partial z)$ is estimated from similarity theory as

$$\frac{\partial\overline{\phi}}{\partial z} = \frac{\Phi_\phi(Z/L)\phi_*}{\kappa Z} \tag{6}$$

where L is the Obukhov length, κ is the von Karman "constant", $\Phi_\phi(Z/L)$ is the specified stability function for variable ϕ and

$$\phi_* \equiv -\frac{\overline{w'(Z,t)\phi'(Z,t)}}{u_*} \tag{7}$$

where u_* is the true surface friction velocity. Substituting Eqs. 6-7 into Eq. 5, we obtain

$$\overline{w'(Z,t)\delta\phi(z')} = \overline{w'(Z,t)z'(t)}\frac{\Phi_\phi(Z/L)\overline{w'(Z,t)\phi'(Z,t)}}{\kappa z u_*}. \tag{8}$$

Dividing this relationship by the flux computed from a stationary platform, the relative error can be written as

$$\overline{w'(Z,t)z'(t)}\frac{\Phi_\phi(Z/L)}{\kappa z u_*}. \tag{9}$$

In the surface layer, Φ_ϕ for heat, moisture and momentum decreases slowly with increasing instability and increases with stability. The principal uncertainty with this "similarity" estimate of the vertical gradient is errors in the similarity relationship with strong stability, advection, and nonstationarity and possible location of the platform within the wave boundary layer (roughness sublayer over land).

5 Displacement flux errors for the aircraft

The displacement flux error depends on record length, method of estimation of the vertical gradient and atmospheric stability. The estimate of the vertical gradient $\partial\overline{\phi}/\partial z$ based on regressing $\phi'(z',t)$ on z for the LongEZ data produces larger vertical gradients than the similarity prediction of the vertical gradient and therefore larger estimates of the displacement error. We will focus on estimates based on similarity theory because the error estimates are less variable. Furthermore, it is not possible to isolate the influence of correlation between turbulence quantities and z' that would contaminate the estimation of the vertical gradient based on the regression method.

5.1 Random and systematic contributions

The dependence of the displacement error on the record length is partly due to the fact that a substantial fraction of the displacement flux error is random. We can theoretically express the displacement error for a particular record as

$$DE = SE + RE \tag{10}$$

where SE is the systematic part of the displacement error and RE is the random part of the displacement flux error. The total displacement error approaches the systematic error as the sample size becomes large, assuming that the sample is homogeneous. This random error is different from the random flux error associated with the estimate of the desired flux for a level platform (first term on the right hand side of Eq. 4). The latter is due to the random distribution of transporting eddies and is always present. We refer to this random error simply as the "random flux error" as opposed to the random part of the displacement error. It is traditionally estimated for

homogeneous records as the standard deviation of the flux, σ_F, divided by the square root of the number of subrecords, N

$$RFE = \frac{\sigma_F}{\sqrt{N}}. \tag{11}$$

For the aircraft, the subrecord width is 200 m, which omits some of the flux for unstable conditions. The intention here is to capture enough subrecords to estimate the standard deviation of the flux. For the present analysis of aircraft data, we evaluate the error term from 2 km records (Section 2), which is smaller than the usual aircraft record length of 10 km or longer. The random flux error and the random part of the flux displacement error both decrease with increasing record length, as will be verified below. In this sense, the following analysis for $2km$ records provides an upper bound for the two random errors.

5.2 Observed distribution

We now examine the behavior of the displacement error normalized by the flux for a stationary platform, as estimated from Eq. 9. The frequency distribution of this relative displacement error does indeed suggest that the random part of the displacement error is substantially larger than the systematic error (Figure 3). The frequency peak of the relative flux displacement error for both heat and momentum fluxes appears to be positive for stable conditions with a value of a few percent, within the uncertainty of the relatively crude resolution of the frequency distribution. The positive values of the relative displacement error correspond to artificial augmentation of the computed flux. Since the expected mean of the random part of the displacement error is zero, this suggests that the relative systematic error is positive with a magnitude of a few percent for stable conditions. Based on the fre-

quency distribution, the relative systematic error for unstable conditions also appears to be positive, but cannot be safely distinguished from zero (Figure 4).

As a quantitative estimate of the displacement error we average the relative displacement error (retaining the sign) for all of the 2 km segments (approximately 560 km of total data) within a stability class. The averaged value of the relative displacement error for stable conditions is +4% for heat and +2% for momentum. The corresponding values are only +0.5% for unstable conditions for both heat and momentum fluxes. For unstable conditions, the relative errors are much smaller, partly due to larger absolute values of the fluxes and partly because the vertical gradients at the aircraft level are generally smaller in the unstable case (thinner surface layer).

As the record length increases from 2 km to 20 km, the random part of the displacement error is expected to decrease by a factor of $1/\sqrt{10}$. For 20 km records (not shown), the magnitude of the relative displacement error is substantially smaller than that for 2 km and rarely exceeds 5%. The relative flux displacement error increases with increasing stability, although the scatter is too large to confidently formulate such a dependence. The relative errors are generally largest for very stable conditions, where the flux magnitudes are small.

5.3 Origin of displacement error

The positive average values of the relative displacement error for stable stratification result from a negative correlation between the atmospheric vertical velocity and the aircraft displacement. The covariance is also generally negative for unstable conditions where the averaged relative displacement error is very small. Theoretically, one might postulate that the covariance should

be near zero because the aircraft displacement, z', would reach its maximum positive value as the updraft switches to downdraft motion, and vice versa. Indeed, the actual correlations between the vertical velocity and the displacement for individual records average only about -0.03, but the correlation is negative for most of the records. The correlation is very small but systematic. The negative correlation suggests an overall lag in the aircraft response to updrafts and downdrafts, which might be influenced by the skewness of the vertical velocity fluctuations, pilot response characteristics and aircraft aerodynamics. We conclude that the flux displacement error for short aircraft records is strongly influenced by the random part of the displacement error but is smaller than the usual random flux error and therefore of limited significance. For longer records, the systematic part of the displacement error is dominant, but is only a few percent of the total flux depending on stability and the transported quantity.

5.4 Random flux error

The random flux error is by definition positive but can be compared to the frequency distribution of the absolute value of the displacement error (Figures 3 and 4, thin solid lines). As an example, the probability of significant relative displacement error greater than 10% is much less than that for the random flux error. The averaged random flux error is about three times greater than the absolute value of the displacement error for both heat and momentum fluxes for stable conditions, and is an order of magnitude greater than the absolute value of the displacement error for unstable conditions. For individual 2-km records, the random flux error is greater than the total displacement error for 90% of the records for both heat and momentum for the stable case while the random flux error is greater than the total

displacement error for all of the records for the unstable case.

6 Buoy displacement flux errors

For ships and buoys, the height of the platform, $z(t)$, may also correlate with $w'(z,t)$ since eddies in the wave boundary layer exhibit phase relationships with the surface waves (e.g. Hare et al., 1997). Eddy correlation measurements are best taken above the wave boundary layer, in the surface layer, where Monin-Obukhov similarity theory potentially applies and such platform-induced errors should be smaller since the vertical displacement of the buoy and the atmospheric vertical velocity should become less correlated.

For a given value of the Obukhov length, the vertical gradients should be larger for the buoy since the buoy measurement level is closer to the surface (6 m compared to about 15 m for the aircraft). However, the relative displacement flux errors are not generally larger for the buoy, partly because both the atmospheric vertical velocities at the buoy observational level and the platform displacements are both generally smaller for the buoy compared to those for the aircraft.

The details of the above results are influenced by the definition of the zero reference height for the buoy. The platform height is separately computed with respect to the distance of the instrument from the mean water height and with respect to the distance from the instantaneous wave field. The latter is affected mainly by short waves since the buoy rides the long waves; that is, z becomes defined as the height above the long waves (swell). The influence of buoy tilt on the distance between the sensor height and wave surface is small. The eddies in the surface layer integrate out the influence of the shorter waves (by definition of the surface layer) so that the correlation

between the turbulent vertical fluctuations and the short waves should be zero. The displacement flux errors for heat are approximately the same in both coordinate systems but the momentum displacement error averages an order of magnitude smaller using the instantaneous height. In the following, we employ height above mean sea level because it is a little easier to interpret, does not depend on the wave riding ability of the buoy and serves as a maximum error estimate.

The correlation between the buoy displacement height and $w'(z',t)$ is larger than that for the aircraft, but still averaging only -0.15. This correlation may be due to the atmospheric streamlines following the long waves. This possibility corresponds to location of the buoy anemometer within the wave boundary layer for the long waves. The displacement flux errors for the buoy depend on wave height through the influence on z' and depend on atmospheric stability through the influence on the vertical gradients. The data were partitioned into intervals of small and large significant wave height (rms of wave height greater than or less than 1.5 m) and further subdivided into stable and unstable classes. Sufficient data were available only for the unstable class. The relative errors for the momentum flux (Figure 5) are shifted towards larger values for the class of large significant wave height. The random part of the error, as indicated by the spread, is less than that for the aircraft (Figures 3-4) because the buoy records are relatively longer (Section 2). The relative displacement error for the heat flux does not show the same sensitivity to the wave height as that for momentum (Figure 5), perhaps because scalar fields do not directly respond to pressure fluctuations. The pressure fluctuations are expected to be larger with large waves. Even for large waves, the relative displacement error for both fluxes are relatively unimportant. The displacement error artificially increases the heat flux and

decreases the momentum flux and, therefore, artificially increases $-z/L$.

7 Heterogeneity terms

The third term on the right hand side of Eq. 4 can be expressed as

$$\frac{\partial \overline{w}}{\partial z}\,\overline{z'(t)\phi'(Z,t)} \tag{12}$$

where we have estimated $\delta w(z')$ from Eq. 1 in terms of the mean vertical gradient and platform displacement z'. For some applications, the horizontal divergence of the wind field might be more easily estimated than the vertical divergence of the vertical velocity. Using incompressible mass continuity, Eq. 12 becomes

$$-\frac{\partial \overline{u}}{\partial x}\,\overline{z'(t)\phi'(Z,t)}. \tag{13}$$

Here, x is assumed to be the primary direction of horizontal divergence $\partial\overline{v}/\partial y \approx 0$.

As an example, consider the case where the platform is a light aircraft and ϕ is the horizontal wind component for offshore accelerating flow, corresponding to horizontal divergence. With a head wind (tail wind), horizontal wind gusts increase (decrease) the lift and z', in which case the correlation is positive (negative) and the flux correction term for momentum is negative (positive). That is, the computed downward momentum flux is artificially enhanced with a headwind and reduced with a tailwind. This term was evaluated from flights perpendicular to the coast by estimating the horizontal gradient of the wind in terms of linear regression over 2 km segments. The term was small for both heat and momentum, generally less than 2% of the

total flux. This term could be potentially important near surface discontinuities, such as flow immediately downstream from the coastline or over heterogeneous land surfaces. However, the flux calculation based on aircraft measurements becomes ambiguous over strong surface heterogeneity in that horizontal variations of the mean flow contaminates the computed turbulent fluctuations. This heterogeneity term could also be large with transient disturbances but significant influences are probably limited to fronts and convective cloud systems. We conclude that this term is small for the heterogeneity encountered in SHOWEX.

Applying Eq. 1 to the fourth term on the right hand side of Eq.4, we obtain the scaling estimate

$$\overline{\delta w(z')\delta\phi(z')} = \frac{\partial\overline{w}}{\partial z}\frac{\partial\overline{\phi}}{\partial z}\overline{z'^2} \tag{14}$$

Again using incompressible mass continuity

$$\overline{\delta w(z')\delta\phi(z')} = -\frac{\partial\overline{u}}{\partial x}\frac{\partial\overline{\phi}}{\partial z}\overline{z'^2} \tag{15}$$

This term can be of either sign depending on whether the flow is accelerating or decelerating. This term is also found to be quite small.

8 Error in mean values

An error in the mean profiles due to platform displacements occurs when the mean gradients are not constant with height. The mean flow measured on a moving platform can be expressed as

$$\overline{\phi(Z + z', t)} = \int_0^\infty \overline{\phi}(Z + z')f(Z + z')d(Z + z') \tag{16}$$

where Z is again the averaged height of the platform and z' is the deviation of the platform height from Z and $f(Z + z')$ is the frequency distribution of the height of the platform. Even if $f(Z + z')$ is a symmetric function of z', the time-average value of $\overline{\phi(Z + z', t)}$ will normally differ from the average at a fixed height, Z, because the time-averaged value of $\overline{\phi}$ is usually a nonlinear function of height. Since the mean shear decreases with height, the mean wind speed on a moving platform will be underestimated. That is, negative $z'(t)$ induces larger artificial fluctuations than positive $z'(t)$. The net effect of this error causes underestimation of the mean wind speed, which in turn cause overestimation of the drag coefficient and roughness length.

An order of magnitude estimate of potential errors due to platform displacement can most easily be constructed for the case of neutral stability with a logarithmic wind profile

$$\overline{u(z,t)} = \frac{u_*}{\kappa} ln \frac{z}{z_o} \tag{17}$$

where z retains traditional meaning and z_o is the aerodynamic roughness length, assumed to be small compared to the observational height. As the simplest possible estimate, assume the aircraft flies 50% of the time at level z_1 and 50% of the time at level z_2, so that the measured average wind speed for sufficiently long record length is

$$\overline{u(Z + z', t)} = \frac{u_*}{2\kappa} (ln \frac{z_1}{z_o} + ln \frac{z_2}{z_o}). \tag{18}$$

Noting that the true averaged wind speed for the average flight level can be expressed as

$$\overline{u(z,t)} = \frac{u_*}{\kappa} ln \frac{(1/2)(z_1 + z_2)}{z_o}, \tag{19}$$

the ratio of the measured wind speed to the true wind speed is

$$\frac{(1/2)(lnz_1 + lnz_2) - lnz_o}{ln(z_1 + z_2) - ln(2z_o)} \tag{20}$$

Incrementally varying z_1 and z_2, corresponding to mean height variations between 4 and 20 m and height differences between 0 and 5 m, the relative platform error is found to be substantially less than 1%. This result was supported by numerically integrating Eq. 16 for the case of a Gaussian distribution of platform errors. Even for a mean observational height of 2 m and displacements of 1m about the mean (corresponding to a 2 m wave height for waves greater than 8 s), the mean wind is underestimated by only 1%.

Defining the error in wind speed as

$$\epsilon \equiv \overline{u(Z + z', t)} - \overline{u(Z)} \tag{21}$$

the drag coefficient estimated from a moving platform is

$$\frac{\overline{w'u'}}{\overline{u(Z,t)}^2 + 2\epsilon\overline{u(Z,t)} + \epsilon^2}. \tag{22}$$

Expanding the denominator in terms of a Taylors expansion, the percentage error in the drag coefficient due to errors in the mean wind is 2ϵ to lowest order. For example, a 1% underestimation of the mean wind leads to a 2% overestimation of the drag coefficient. We conclude that the effect of platform displacement on the mean wind and drag coefficient is not important. The percentage error for the mean shear will be substantially larger, particularly for larger values of z and smaller values of the difference between the observational levels used to estimate the shear.

9 Conclusions

We have studied the impact of errors due to vertical displacement of platforms resulting from contamination of the computed turbulent fluctuations by mean vertical gradients. Aircraft platform fluctuations for the present data lead to small overestimation of the heat and momentum fluxes for stable conditions and unimportant errors for unstable conditions. For typical record lengths, the magnitude of the displacement flux error is generally smaller than the usual random flux error, where the latter remains nonzero even for stationary platforms. Both random errors are reduced by increasing record length.

The displacement flux error can be theoretically partitioned into a random part (not to be confused with the usual random flux error) and a systematic part. The flux displacement error for short aircraft records is strongly influenced by the random part of the displacement flux error, which is smaller than the usual random flux error. For longer aircraft records, the random part of the displacement flux error decreases and the displacement flux error approaches the small systematic part of the error, typically a few percent of the total flux for stable conditions and less than one percent for unstable conditions. The systematic error tends to increase with stability. The general unimportance of the displacement error for the LongEZ is encouraging since this small aircraft is displaced more by atmospheric vertical velocity fluctuations compared to larger aircraft. Larger aircraft are unable to fly as close to the sea surface and are therefore less suitable for estimating surface fluxes in thin stable boundary layers over the sea. For flight levels closer to sea surface, the flux displacement error is expected to be larger because of larger vertical gradients. The present investigation considered only marine environments. Aircraft displacement errors may be greater over rougher land

surfaces or more strongly heated surfaces where aircraft displacements are larger. Unmanned aircraft may suffer larger platform displacement errors because of larger vertical displacements.

Compared to the aircraft, the buoy errors would be enhanced by stronger gradients at the lower observational levels of the buoy, but are reduced by small magnitudes of the buoy displacement and the small vertical velocities close to the surface. The displacement flux error for the buoy becomes marginally significant only for large wave heights where it averages a few percent.

Acknowledgments

The helpful comments of the reviewers are gratefully acknowledged. This material is based upon work supported by Grants N00014-97-1-0279 and N00014-01-1-0084 from the Office of Naval Research, Marine Meteorology and N00014-97-1-0348 from the Office of Naval Research, Coastal Dynamics.

References

Crescenti, G.H., T.L. Crawford, and E.J. Dumes, Data Report: Long EZ(N3R) participation in the 1999 shoaling waves experiment(SHOWEX) pilot study. NOAA Technical Memorandum ERL ARL- 232, Silver Spring, MD, 86, 1999.

Edson, J., A. Hinton, K. Prada, J. Hare, and C. Fairall, 1998: Direct covariance flux estimates from mobile platforms at sea. *J. Atmos. Oceanic Tech.* , **15**, 547-562.

French J.R., G.H. Crescenti, T.L. Crawford and E.J. Dumas, Long EZ participation in the 1999 shoaling waves experiment (SHOWEX), NOAA Data Report OAR ARL-20, Silver Spring, MD, 51, 2000.

Graber, H.C., E.A. Terray, M.A. Donelan, W.M. Drennan, J. Van Leer and D.B. Peters, 2000: ASIS – A new air-sea interaction spar buoy: design and performance at sea. *J. Atmos. Oceanic Tech.* , **17**, 708-720.

Hare, J. E., T. Hara, J. B. Edson, and J. M . Wilczak, 1997: A similarity analysis of the structure of airflow over surface waves. *J. Phy. Oc.*, **27**, 1018-1037.

Lenschow, D. H., 1973: Two examples of planetary boundary layer modification over the Great Lakes. *J. Atmos. Sci.*, **30**, 568-581.

Lenschow, D. H., 1986: Aircraft Measurements in the Boundary Layer. A chapter in *Probing the Atmospheric Boundary Layer*, edited by D. H. Lenschow, American Meteorological Society, Boston, MA, 39–55.

Mahrt, L., 1998: Flux sampling strategy for aircraft and tower observations. *J. Atmos. Oceanic Tech.* , **15**, 416-429.

Mahrt, L., D. Vickers, J. Sun, T. Crawford, G. Crescenti, and P. Frederickson, 2001: Surface stress in offshore flow and quasi-frictional decoupling. *J. Geophys. Res.*, **106**, 20,629-20,639.

Mann, J. and D. H. Lenschow, 1994: Errors in airborne flux measurements. *J. Geophys. Res.*, **99**, 14,519-14,526.

Massman, W. J., 2000: A simple method for estimating frequency response corrections for eddy covariance systems. *Agric. For. Meteorol.* , **104**, 185-198.

Moore, C. J., 1986: Frequency Response Corrections for Eddy Correlation Systems, *Boundary-Layer Meteorol.*, **37**, 17-35.

Sun, J., Vandemark, D., Mahrt, L., Vickers, D., Crawford, T., and Vogel, C., 2001: Momentum Transfer over the Coastal Zone. *J. Geophys. Res.*, **106**, 12,437-12,448.

Vickers, D. and Mahrt, L., 1997: Quality control and flux sampling problems for tower and aircraft data, *J. Atm. and Oc. Tech.*, **14**, 512-526.

10 Figure Legends

Figure 1. Geometry of superficial fluctuations due to vertical platform displacement in the presence of mean vertical gradients. The upper panel defines z' and Z for a hypothetical times series of platform height. The lower panel illustrates artificial fluctuations generated by vertical platform displacement

in the presence of mean vertical gradients.

Figure 2. Examples of vertical displacement of the LongEZ for unstable conditions (a), stable conditions (b) and for the ASIS buoy for slightly stable conditions with 13 ms^{-1} mean wind and a large significant wave height of 4 metres (c).

Figure 3. The frequency distribution of the relative displacement error (thick solid), the absolute value of the relative displacement error (thin solid) and the random flux error estimated from Eq. 11 (dashed) for the LongEZ aircraft data for stable conditions for heat fluxes (a) and momentum fluxes (b).

Figure 4. The frequency distribution of the relative displacement error (thick solid), the absolute value of the relative displacement error (thin solid) and the random flux error estimated from Eq. 11 (dashed) for the LongEZ aircraft data for unstable conditions for heat fluxes (a) and momentum fluxes (b).

Figure 5. The frequency distribution for the relative displacement flux error for the ASIS buoy for unstable conditions for heat (upper panel) and momentum (lower panel) where the solid line represents the class of large significant wave height and the dashed line represents the class of small significant wave height.

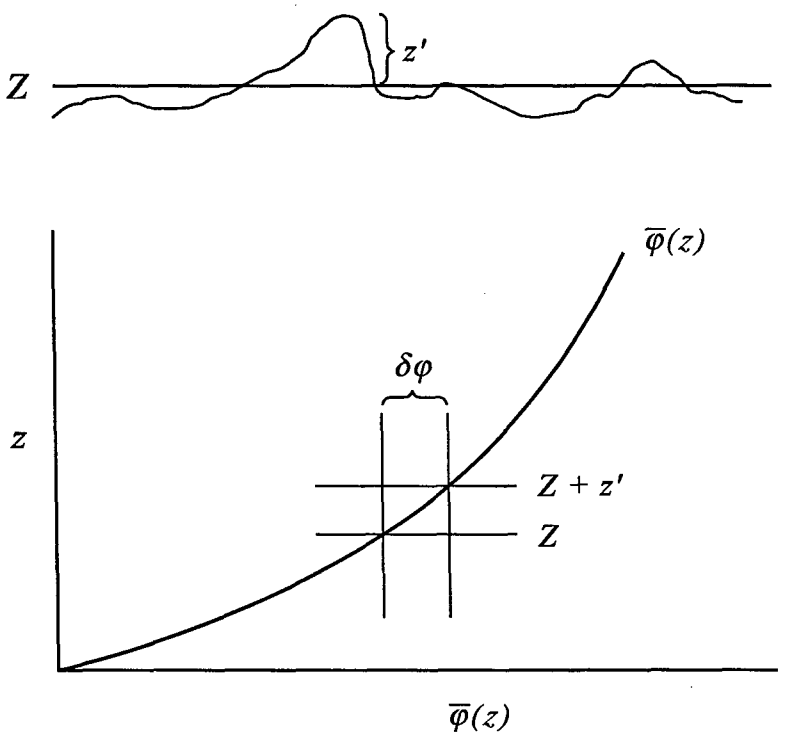

Figure 1:

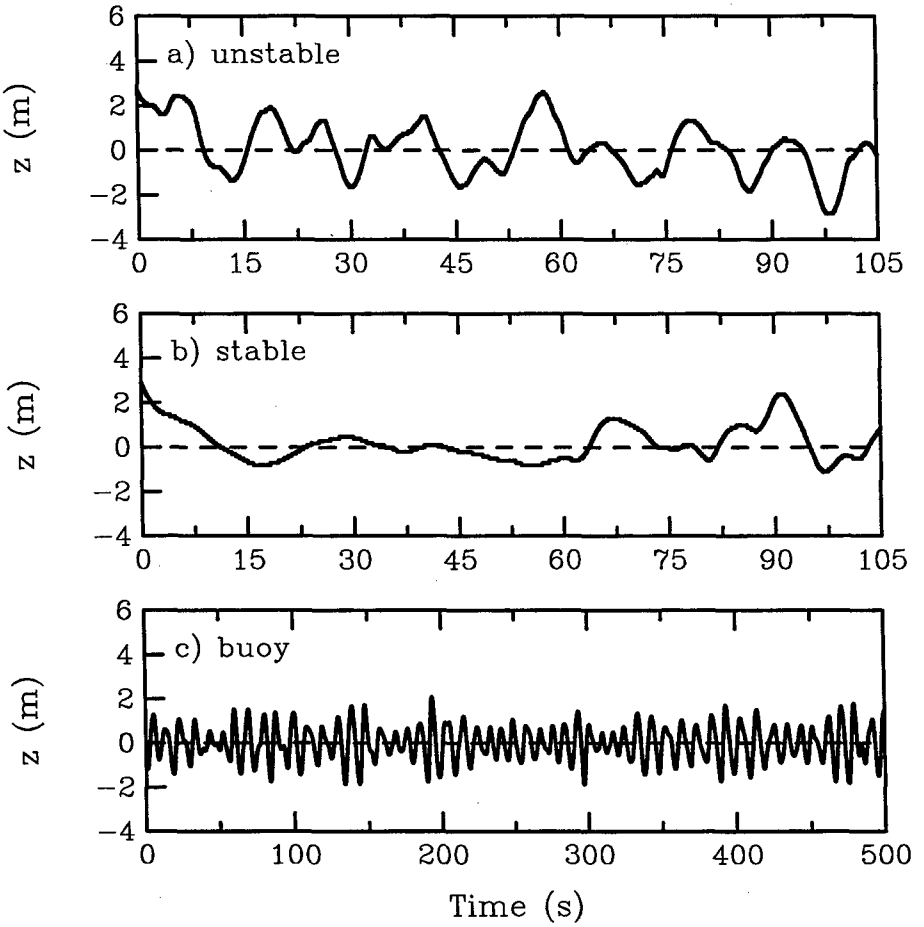
a) unstable
b) stable
c) buoy
z (m)
Time (s)
6
4
2
0
−2
−4
0
15
30
45
60
75
90
105
100
200
300
400
500

Figure 2:

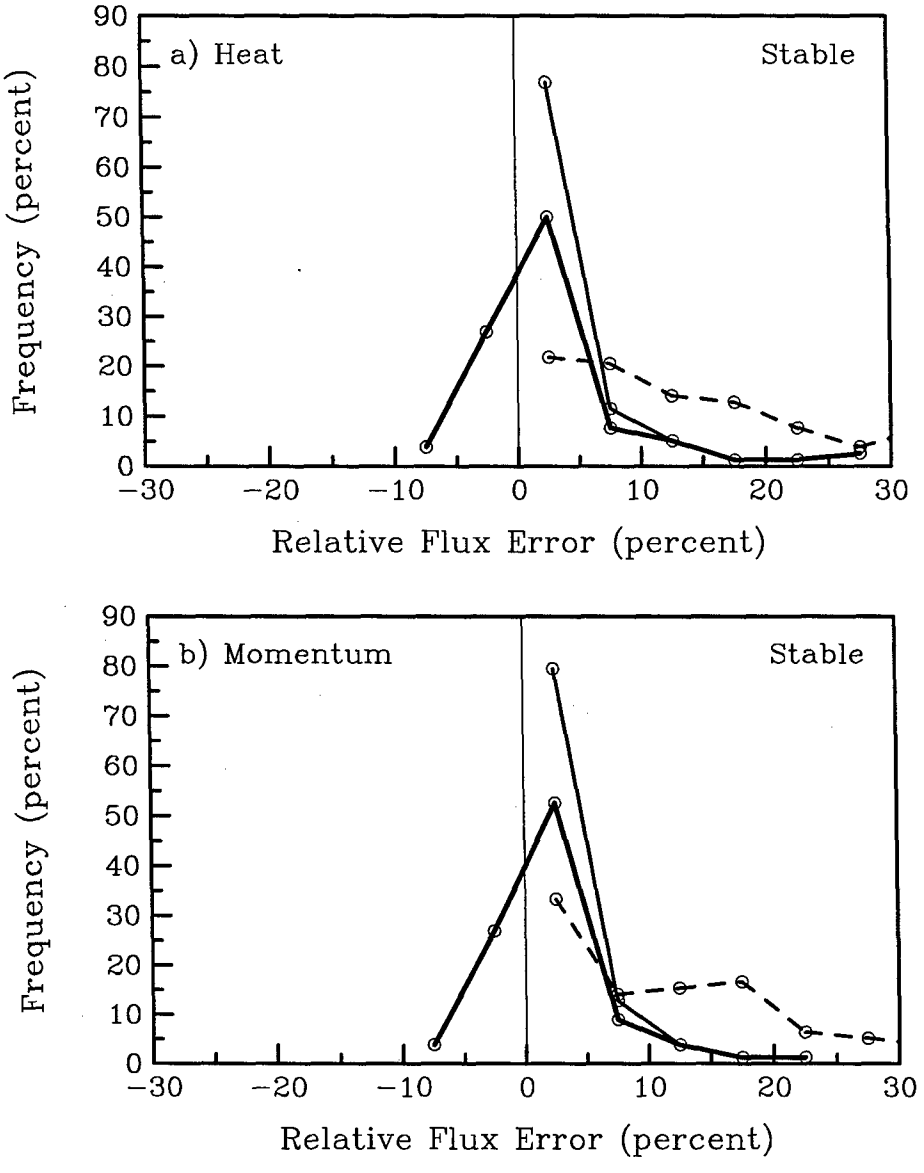
a) Heat
Stable
Frequency (percent)
Relative Flux Error (percent)
b) Momentum
Stable
Frequency (percent)
Relative Flux Error (percent)

Figure 3:

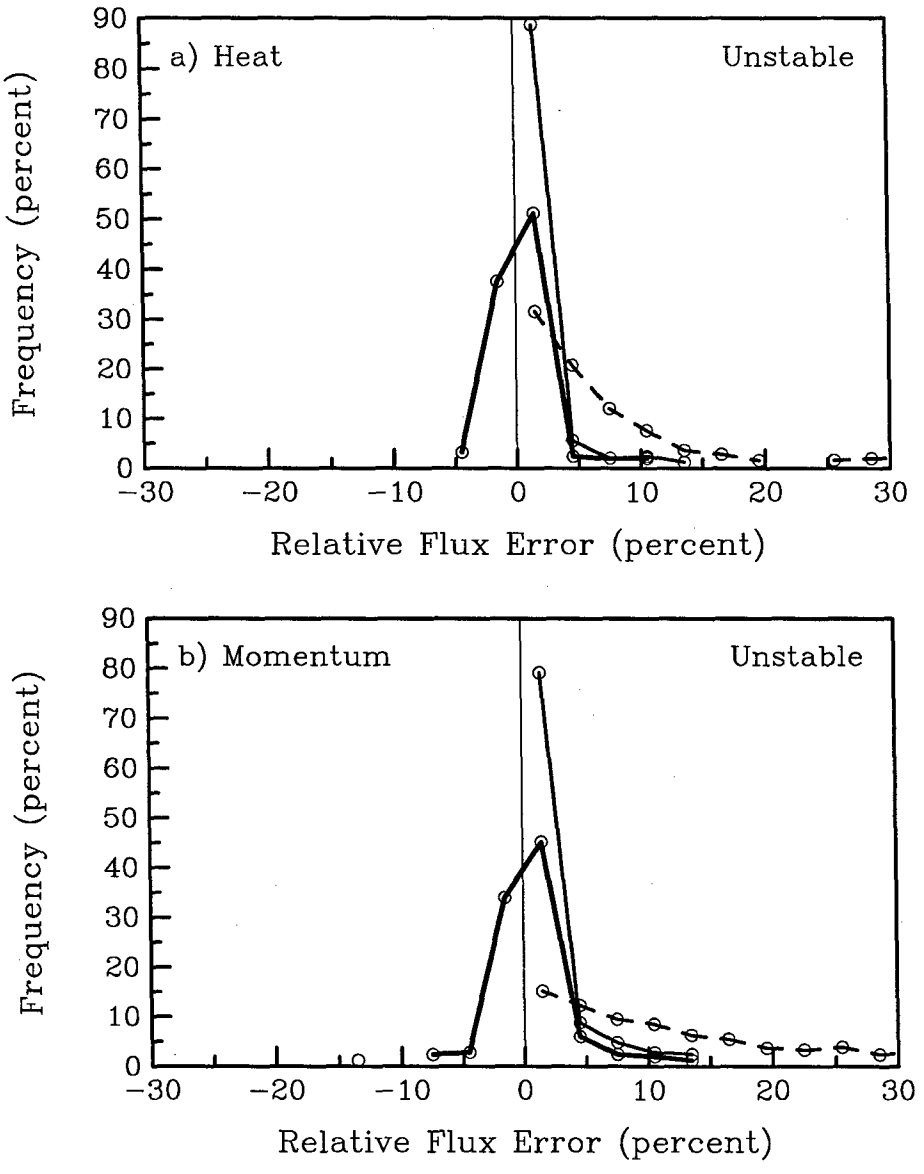
a) Heat
Unstable
Frequency (percent)
Relative Flux Error (percent)
b) Momentum
Unstable
Frequency (percent)
Relative Flux Error (percent)

Figure 4:

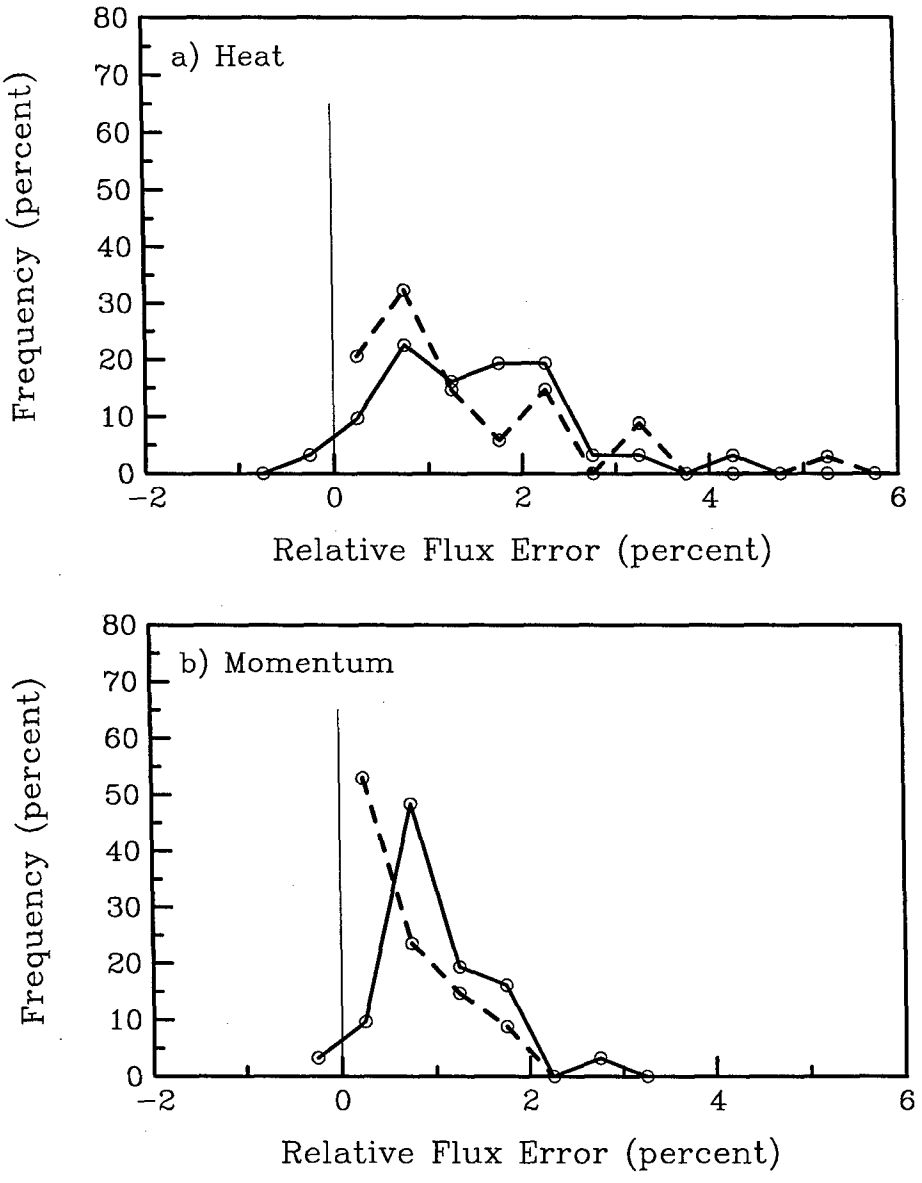
a) Heat
Frequency (percent)
Relative Flux Error (percent)
b) Momentum
Frequency (percent)
Relative Flux Error (percent)

Figure 5:

FLOW ADJUSTMENTS ACROSS SEA-SURFACE TEMPERATURE CHANGES

L. MAHRT (mahrt@coas.oregonstate.edu), DEAN VICKERS and ERIN MOORE
College of Oceanic and Atmospheric Sciences, Oregon State University, Corvallis, OR 97331, U.S.A.

Abstract. The adjustment of airflow across sea-surface temperature changes is examined using aircraft eddy-correlation data. Major features of the observed flow adjustment are not included in the theory of internal boundary layers. However, the data sample size and coverage are not sufficient to accurately quantify the additional influences. With flow from warm water over cooler water, substantial turbulence intermittently develops above the newly formed surface inversion layer. The corresponding, spatially-averaged, downward momentum flux is stronger than that close to the surface.

With stably stratified flow over modest increases of sea-surface temperature, reduction of stratification can trigger episodic shear generation of turbulence. In these cases, the primary role of increasing surface temperature in the downwind direction is to induce shear generation of turbulence. With larger increases of surface temperature, upward heat flux generates turbulence, warms the air and generates a significant horizontal gradient of hydrostatic pressure. This contribution to the pressure field appears to strongly modify the flow. Major inadequacies in existing data and future needs are noted.

Keywords: Internal boundary layer, SST front, Heterogeneity, Secondary circulations, Mesoscale

1. Introduction

Airflow over a surface temperature discontinuity often induces an internal boundary layer as the air near the surface adjusts to the new surface conditions. Unstable internal boundary layers, as with flow of cool air over warm water, have been studied in detail and are reasonably well understood, particularly on the mesoscale where the internal boundary layer is capped by an inversion or entrainment zone (e.g., Steyn and Oke, 1982; Garratt, 1990; Attié and Durand, 2003). On smaller horizontal scales where such a capping inversion is not yet formed, the top of the internal boundary layer can be defined in terms of the top of bent over thermals rising into cooler air (Mahrt, 2000; Klipp and Mahrt, 2003). In this region just downwind from the surface temperature increase, the vertical transfer may still be influenced by upwind dynamics (Andreas and Cash, 1999).

2

Stable internal boundary layers forming in flow of warm air over cooler surfaces are even more complex and less understood (Garratt, 1987; Vickers et al., 2001; Sun et al., 2001). The stable internal boundary layer can be difficult to define in terms of turbulence structure, since the turbulence often increases with height and reaches a maximum above the surface stable layer (Mahrt 2000). The decoupled flow above the surface stable layer accelerates and a low-level wind maximum, similar to the nocturnal jet, may form (Smedman et al., 1995; Vihma and Brümmer, 2002).

The present study analyzes aircraft eddy correlation data collected in flow over changes of sea surface temperature. A number of important features are identified, which are not included in the above studies. For example, small increases of surface temperature in the downwind direction can lead to thermally-induced shear generation of turbulence without development of a convective boundary layer (Section 3.1). The local pressure gradient associated with the horizontal temperature gradient can strongly alter the flow (Section 3.2). With decrease of surface temperature and formation of a stable surface inversion layer, significant turbulence intermittently develops above the surface inversion layer (Section 4). Inadequacies of the present data and future needs are outlined in Section 5.

2. Data

This study analyzes data taken off the coast of the Outer Banks of North Carolina, USA during the Shoaling Wave Experiment (SHOWEX; Crescenti et al., 1999, French et al., 2000 and Sun et al., 2001) conducted 11 November-5 December 1999. Here we analyze data collected by the LongEZ (N3R) aircraft, including the three wind components, temperature and humidity at a rate of 50 samples per second. With an approximate air speed of 55 m s^{-1}, this sampling rate corresponds to a sample width of about 1 m.

Three flights were carried out perpendicular to shore about 100 km east of the coast over the western edge of the Gulf Stream. Passes were flown at two levels in the lowest 100 m and supplemented with aircraft soundings. The western edge of the Gulf Stream was locally directed more or less parallel to the coast (approximately south southwest to north northeast) during the flights. The sea-surface temperature (SST) increases by typically 4 °C across the western boundary of the Gulf Stream (Figure 1). On 19 November, when the air flow was approximately parallel to the SST front, the front is particularly sharp (Figure 1). On 20 November with a westerly wind component across the Gulf

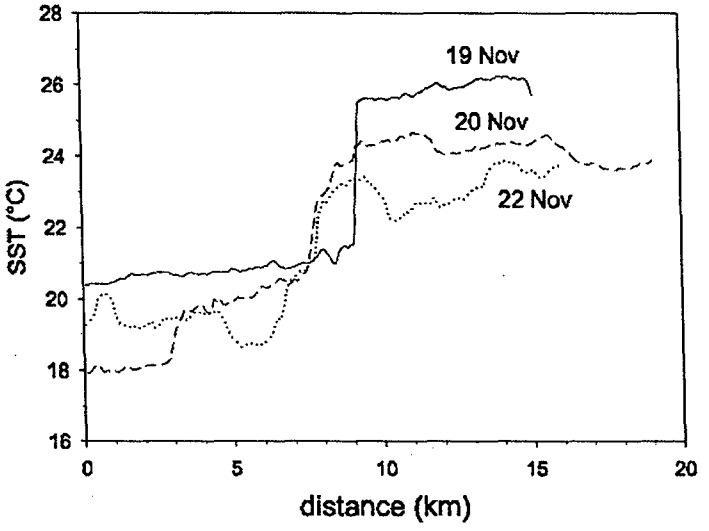

Figure 1. The horizontal variation of the SST across the western edge of the Gulf Stream along the east-west flight track on 19, 20 and 22 November.

Stream, the SST front is not as sharp and a secondary SST front is located about 5 km west of the main front with a temperature increase of about 1.5 °C (Figure 1). This secondary front occurs as a local temperature maximum when viewed from the 8-m flight track instead of the 33-m flight level, which was slightly displaced horizontally from the track at 33 m. On 22 November, the wind is easterly and the SST front is not very sharp with multiple small-scale variations.

Air-sea temperature differences are expressed in terms of a local potential temperature ($T(z) + 0.01\ z$ °K m^{-1}), where z is the aircraft altitude above the sea surface in metres. Unfortunately, the radiometrically-measured sea-surface temperature is not very accurate due to drift of the reference temperature of the Everest Interscience Inc. 4000.4GL. Absolute errors may be as large as 1°C. Therefore, the radiometer measurements will be used only to qualitatively determine the spatial pattern of the sea-surface temperature.

Order of magnitude estimates of the buoyancy and shear generation of turbulence energy will be made. The shear generation of turbulence can be expressed as

$$\frac{u_*^3 \phi_m}{\kappa z} \tag{1}$$

where ϕ_m is the nondimensional shear, estimated as a function of z/L from Monin-Obukhov similarity theory. The fluxes and the friction velocity have been estimated from the eddy correlation measurements

using a 2-km averaging window. The friction velocity is computed from both the along-wind and cross-wind components as is the magnitude of the momentum flux used in the Obukhov length. Fluxes at the aircraft level may be different than the surface values, particularly for stable conditions. While similarity theory may be only a crude approximation, we believe it to be more accurate than estimating the actual shear near the surface using winds from the two aircraft levels.

3. Flow from cool to warmer water

3.1. Upwind from the SST front

On 20 November, southwesterly flow of cooler air over the warmer water leads to development of a convective internal boundary layer. Based on profiles of potential temperature and moisture provided by an aircraft sounding upwind from the SST front near the west end of the aircraft track, the depth of the stable inversion layer is about 70 m. The turbulence upwind from the SST front near the surface (8-m level) is relatively weak (Figure 2, lower panel). The friction velocity is typically between 0.05 and 0.10 m s^{-1}. At the 33-m level, the turbulence is even weaker (Figure 2, upper panel) and the friction velocity is typically about 0.02 m s^{-1}, considered to be zero within observational error. These values suggest a thin turbulent boundary layer, shallower than 30 m and significantly shallower than the surface inversion layer. The depth of the surface inversion layer was well defined in terms of vertical profiles of the potential temperature and specific humidity constructed from aircraft slant soundings.

The data at 8 m show patches of enhanced turbulence, sometimes associated with small local increases of the SST upwind from the main SST front. Generally this local enhancement of turbulence is associated with an increase of momentum flux without observable upward heat flux. The example record in Figure 3 shows three types of turbulence events. With the first type, significant turbulence and downward momentum and downward heat flux develop at the 10-km location (Figure 3) without any SST change. This type of event did not occur with this strength in the other records. In the second type of turbulence event, very weak upward heat flux and increase of turbulence occur at a horizontal distance of 17 km (Figure 3) where the SST increases by about 1° C. Significant turbulence but no upward heat flux develops at 22 and 25 km (Figure 3), where the SST gradually increases just west of the main SST front. Upward heat flux develops just downwind from this event.

Considering all five records at the 8-m level upwind from the main SST front, eight events were defined where u_* locally exceeds 0.1 m s^{-1}. Five of these events were associated with an increase of SST of about 1 °C or greater. Since the SST increases occupy a small fraction of the flight path, we conclude that locations of SST increases are preferred locations for turbulence development. For four of the five events, buoyancy generation of turbulence was negligible or at least an order of magnitude smaller than the shear generation of turbulence. In the other case, the buoyancy generation was as large as the shear generation. For cases of turbulence development without upward heat flux, the turbulence could be generated by shear instability induced by reduction of the positive air-sea temperature difference and corresponding reduction of the bulk Richardson number. Since the air temperature changes much more slowly than the sea-surface temperature, small-scale changes of the air-sea temperature differences track closely with small-scale changes of the sea-surface temperature. While these observations are suggestive of the importance of thermally-induced shear generation, the number of events is far too small to form definite conclusions.

For three of the five passes at the 33-m level, the increased turbulence upwind from the main SST front leads to local cooling of the air of about 0.5 °C (e.g., Figure 2, 10 km point, upper panel). This cooling is presumably due to mixing of cooler air from near the surface upward to the aircraft level.

3.2. Thermally-induced pressure gradient

The heat flux downwind from the SST front is usually upward but does not become strong at the aircraft level until several kilometers further downwind (Figure 4). The increase of heat flux on this day lags the increase of momentum flux by several km at the 33-m flight level (Figure 4), with considerable variability between passes. As a result, the turbulence in the airflow immediately downwind from the main SST front is generated primarily by shear. This could correspond to the "mixed" regime reported by Andreas and Cash (1999) where the upwind dynamics still influences the vertical transfer immediately downwind from a surface temperature increase. The buoyancy generation could act more as a catalyst for strong shear generation of turbulence. As the flow moves farther downwind from the SST front over the warmer sea surface, the convective turbulence strengthens and deepens.

The warming of the air over the warmer water leads to a significant horizontal temperature gradient over the first 5 km downwind from

6

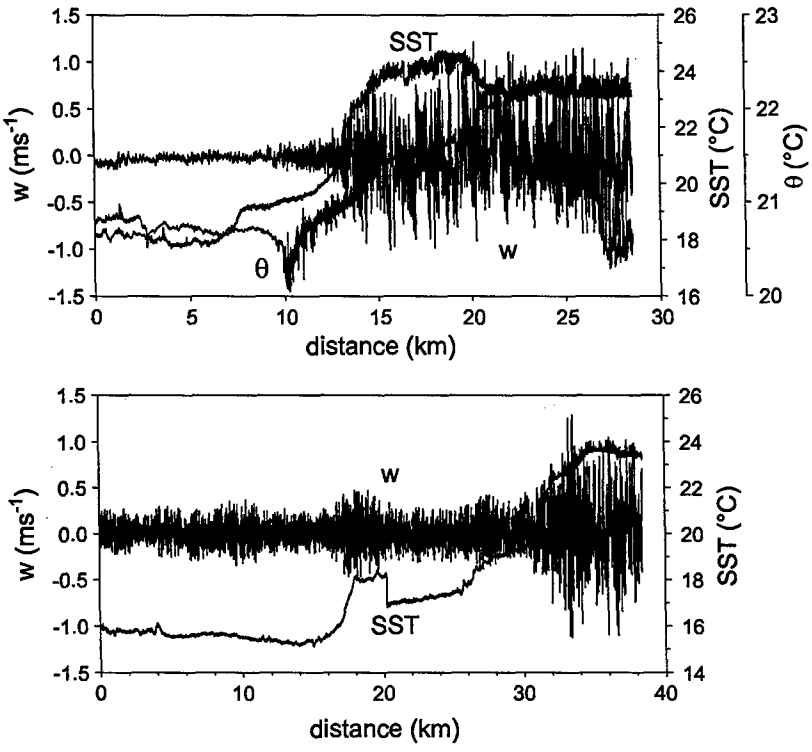

Figure 2. The horizontal variation of SST, air potential temperature (θ on an expanded vertical scale) and vertical velocity (w) for an individual pass at 33 m (upper panel) and an individual pass at 8 m (lower panel) on 20 November. The flow is from left to right.

the SST front (Figure 5, upper panel). The westerly flow component accelerates across the region of strong horizontal temperature gradient toward the warmer air (Figure 5, 8-14 km). Such horizontal acceleration is consistent with a local horizontal pressure gradient due to horizontal variation of the air temperature. This contribution to the pressure field corresponds to lowest surface pressure under the warmest air. That is, we hypothesize a thermal low pressure system, which is superimposed on the larger-scale pressure gradient.

Using the sounding data together with the two horizontal flight levels, the thermally-induced pressure gradient along the flight track was estimated by vertically integrating the hypsometric equation between the surface and the 100-m level, the perceived maximum depth of significant horizontal temperature variation. The height dependence

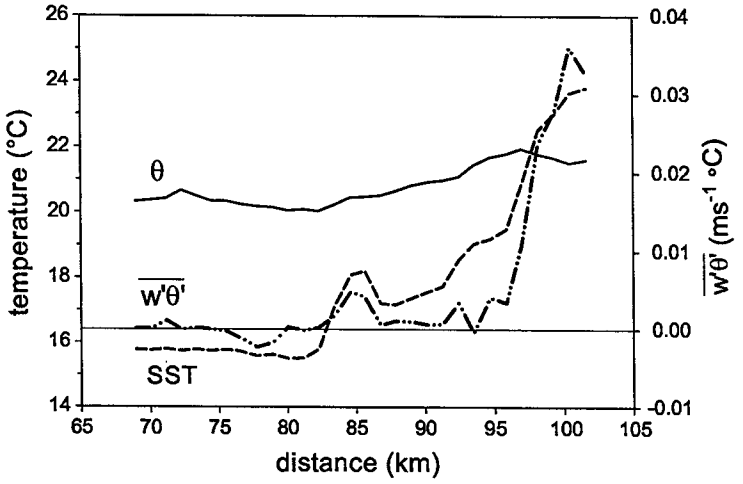

Figure 3. An example of 1-km fluxes for a single pass at 8 m on 20 November.

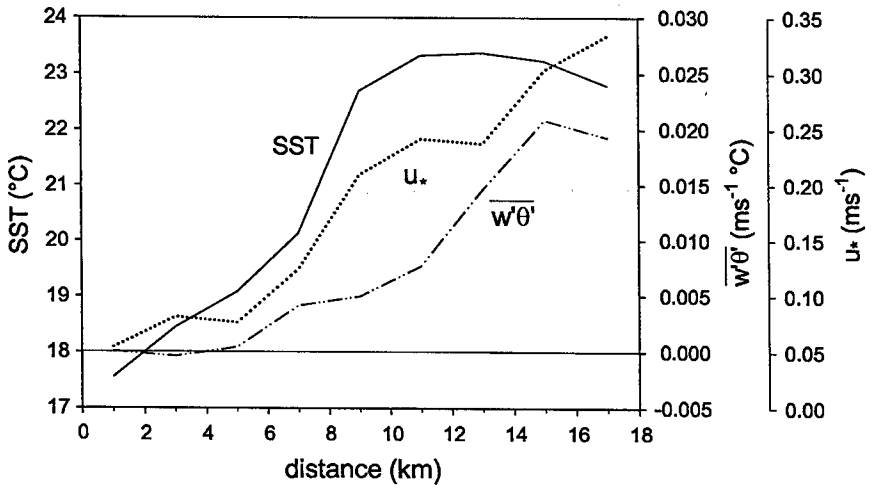

Figure 4. The spatial variation of the SST, friction velocity and heat flux at 33 m near the main SST front on 20 November. The values are composited over the 5 passes. The compositing causes some spatial spreading because the individual records are not perfectly aligned with respect to the SST front. The flow is from left to right.

8

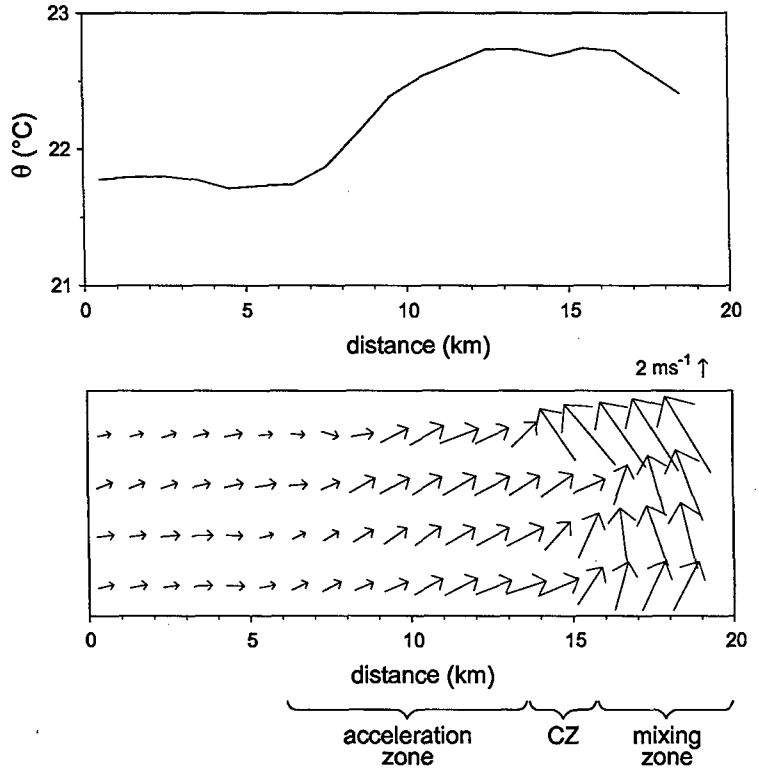

Figure 5. The along-flight variation of the composited potential temperature at the 33-m level on 20 November (upper panel) and the 1-km averaged wind vectors at 33 m (lower panel) for 4 sequential passes over the same track, the first pass is at the top and so forth. A unit vector of 2 m s $^{-1}$ is shown above the right hand corner. The vectors are plotted as a planview with north directed upward and east directed to the right. The bracketing delineates the zone where the flow is accelerated toward the warmest air, the convergence zone (CZ) and the zone where strong southerly momentum is convectively mixed downward toward the surface.

of the horizontal temperature gradient was fit to an exponentially decaying function with the amplitude based on the lowest flight level and a decay height of 100 m. The thermally-induced pressure gradient is also estimated with a simpler approach (Equation 9 in Mahrt, 1982) of the form

$$\frac{g}{\Theta} h \frac{\partial[\theta]}{\partial x}, \tag{2}$$

where $[\theta]$ is the vertically integrated potential temperature from the surface up to a constant depth, h, and Θ is a scale value of the poten-

tial temperature. The vertically- and horizontally-averaged potential temperature for both sides of the SST front were determined from both aircraft levels and the aircraft soundings. The order of magnitude of the thermally-induced pressure gradient determined by the two methods is estimated to be between 10^{-4} and 10^{-3} m s $^{-2}$. The magnitude of the Coriolis term near the surface in the acceleration zone (Figure 5) is approximately 4×10^{-4} m s^{-2}. The magnitude of the large-scale pressure gradient term is estimated by assuming that the southerly flow above the surface flow is approximately geostrophic. The value of the large-scale pressure gradient term is then estimated to be about 8×10^{-4} m s^{-2}. The other terms in the momentum budget could not be estimated with adequate accuracy to form even order of magnitude estimates. These calculations indicate that the thermally-induced horizontal pressure gradient is important. However, errors in the estimation of the thermally-induced pressure gradient are probably large because of limited information on the vertical structure over the warm side of the SST front. However, the sign of the thermally-induced horizontal pressure gradient near the surface is consistent with acceleration of the westerly flow component across the region of large horizontal temperature gradient.

The southerly flow observed at the surface east of the convergence zone (Figure 5) is probably due to strong downward mixing of stronger southerly flow. This strong downward mixing is caused by the buoyancy-driven turbulence. The aircraft soundings show stronger southerly flow at higher levels over the entire region, presumably driven by the large-scale pressure gradient. This downward mixing does not eliminate the westerly flow near the surface in the region of strong horizontal temperature gradient (acceleration zone, Figure 5). Apparently, west of the convergence zone but still over the warm water, the local thermally-induced horizontal pressure gradient is more important than the downward mixing of momentum.

4. Stable case

A stable inversion layer develops on 22 November when easterly flow advects warm air from over the warmer water to over the cooler water. The generally weak upward heat flux over the warmer surface on this day changes to weak downward heat flux downwind from the SST front over cooler water. The magnitude of the downward momentum flux at the 9-m flight level decreases downwind over the cooler water accompanied by considerable modulation.

10

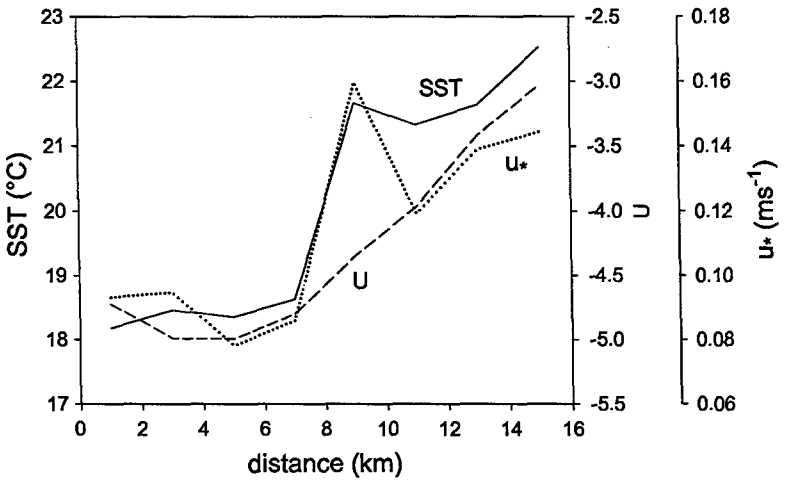

Figure 6. The spatial variation of 2-km averages of SST, u_* and the westerly wind component (U), here negative, for flow from warm water over cooler water on 22 November for the 9-m flight level. Values have been composited over 6 passes. The flow is from right to left.

The spiral aircraft sounding taken over the cool water shows a surface stable layer forming downwind of the SST front up to about 50 m above the surface at the sounding location. A warmer residual layer overrides the stable surface layer and extends from 50 m up to about 300 m above the surface. At the 90-m flight level within the residual layer, the turbulence decays rapidly downwind from the SST front, but dramatically increases at a patch of turbulence about 2 km wide for each of the two passes. The events are characterized by large u_* values, exceeding 0.3 m s $^{-1}$. For the single pass at 280 m, a similar turbulent burst is observed. The bursts occur at different relative positions with respect to the main SST front and do not seem related to variations of SST downwind from the main front. They are apparently driven by shear above the surface inversion. As a result of these events, the spatially-averaged turbulence energy and momentum flux are larger at the 90-m level than at the 9-m level, albeit, random flux errors are large. Since the turbulence and stress increase with height, the turbulence is no longer surface-based in the sense that the primary source of turbulence is at higher levels. Based on aircraft data across an open ocean sea-surface temperature front, Friehe et al. (1991) found that the stress decreased with height even on the stable side over the

cooler water, although the SST front was weaker than in the present study.

5. Conclusions and discussion

With flow of warm air over cooler water, relatively strong intermittent bursts of downward transport of momentum occur above the newly formed surface inversion over the cooler water. As a result, the magnitude of the spatially-averaged downward momentum flux increases with height, although flux sampling errors are large.

With modest increases of surface temperature, significant turbulence and momentum flux sometimes develop even if the airflow remains stable and the heat flux is small. Apparently, the reduced stratification allows development of significant shear generation of turbulence. Here, the increase of surface temperature in the downwind direction acts more as a catalyst for shear generation of turbulence in contrast to the convective internal boundary layer where direct buoyancy generation of turbulence is large. More substantial increases of surface temperature, as occurs at the main SST front, lead to significant buoyancy generation of turbulence and warming of the air downwind from the surface front. The resulting horizontal temperature gradient contributes to a local hydrostatic pressure gradient, which accelerates flow towards the warmer air.

The triggering of shear generation of turbulence by modest increases of surface temperature in the flow direction may be much more frequent than the development of convective internal boundary layers downwind from large surface temperature changes. Surface temperature changes over land and sea are often not sufficiently strong to change the sign of the stratification and surface heat flux.

The spatial coverage and sample size in the present data are inadequate for accurate quantitative analysis of the momentum budget and turbulence kinetic energy budgets. Evaluation of the full dynamics of flow past surface temperature changes requires observations of the horizontal variation of the vertical structure of the wind, temperature and fluxes with adequate sampling at each point. This demanding task would be served by a large number of aircraft passes at multiple levels using multiple aircraft and deployment of multiple towers along the track. Otherwise, the interpretation of the data must rely heavily on inferences, as in the present study.

12

Acknowledgements

This paper is dedicated to Tim Crawford who died during a LongEZ flight while collecting low-level eddy correlation data near the Woods Hole Oceanographic Institute, USA. Tim Crawford collected the data analyzed in this paper. Thanks to Tim's unequaled dedication, the data are indeed unique.

We thank Don Lenschow, Cheryl Klipp, Ralph Foster, John Garratt and one anonymous reviewer for comments on the manuscript. This research was funded by the Office of Naval Research, Marine Meteorology, Grants N000149710279 and N00014-01-1-0084

References

Andreas, E. L., and Cash, B. A.: 1999, 'Convective Heat Transfer over Wintertime Leads and Polynyas', *J. Geophys. Res.* **104**, 25,721-25,734.

Attié, J.-L., and Durand, P.: 2003, 'Conditional Wavelet Technique Applied to Aircraft Data Measured in the Thermal Internal Boundary Layer during Sea-Breeze Events', *Boundary-Layer Meteorol.* **106**, 359-382.

Crescenti, G. H., Crawford, T. L., and Dumas, E. J.: 1999, *Data Report: LongEZ (N3R) Participation in the 1999 Shoaling Waves Experiment (SHOWEX).* Spring Pilot Study, NOAA Technical Memorandum ERL ARL-232, Silver Spring, MD, 86pp.

French, J. R., Crescenti, G. H., Crawford, T. L., and Dumas, E. J.: 2000, *LongEZ (N3R) Participation in the 1999 Shoaling Waves Experiment (SHOWEX),* NOAA Data Report OAR ARL-20, Silver Spring, MD, 51pp.

Friehe, C. A., W. J. Shaw, D. P. Rogers, K. L. Davidson, W. G. Large, S. A. Stage, G. H. Crescenti, S. J. S. Khalsa, G. K. Greenhut, and F. Li: 1991, 'Air-sea fluxes and surface layer turbulence around a sea-surface temperature front', *J. Geophys. Res.* **96**, 8593-8609.

Garratt, J.R.: 1987, 'The stably stratified internal boundary layer for steady and diurnally varying offshore flow', *Boundary-Layer Meteorol.* **38**, 369-394.

Garratt, J.R.: 1990, 'The Internal Boundary Layer - A Review', *Boundary-Layer Meteorol.* **50**, 171-203.

Klipp, C. and Mahrt, L.: 2003, 'Conditional Analysis of an Internal Boundary Layer', *Boundary-Layer Meteorol.* **108**, 1-17.

Mahrt, L.: 1982, 'Momentum balance of gravity flows', *J. Atmos. Sci.* **39**, 2701-2711.

Mahrt, L.: 2000, 'Surface Heterogeneity and Vertical Structure of the Boundary Layer', *Boundary-Layer Meteorol.* **96**, 33-62.

Smedman, A., Bergström, H., and Högström, U.: 1995, 'Spectra, Variances and Length Scales in a Marine Stable Boundary Layer Dominated by a Low Level Jet', *Boundary-Layer Meteorol.* **76**, 211-232.

Steyn, D. G. and Oke, R. R.: 1982, 'The Depth of the Daytime Mixed Layer at Two Coastal Sites: A Model and its Validation', *Boundary-Layer Meteorol.* **24**, 161-180.

Sun, J., Vandemark, D., Mahrt, L., Vickers, D., Crawford, T., and Vogel, C.: 2001, 'Momentum Transfer over the Coastal Zone', *J. Geophys. Res.* **106**, 12,437-12,488.

Vickers, D., Mahrt, L., Sun, J., and Crawford, T.: 2001, 'Structure of Offshore Flow', *Mon. Wea. Rev.* **129**, 1251-1258.

Vihma, T. and Brümmer, B.: 2002, 'Observations and Modelling of the On-Ice Air Flow over the Northern Baltic Sea', *Boundary-Layer Meteorol.* **103**, 1-27.